

Sound power radiation due to an isolated airfoil in a turbulent stream

Vincent P. Blandeau, Phillip F. Joseph and Gwénaél Gabard

Fluid Dynamics and Acoustics group, ISVR, University of Southampton, Southampton, UK

PACS: 43.28.-g 43.28.Ra

ABSTRACT

This paper presents an analytical study of the sound power radiated from a two dimensional flat plate airfoil in a turbulent stream. A classical approach for describing analytically the response of a flat plate, with a finite chord, to the impingement of turbulence is extended to be valid at all frequencies. Analytical asymptotic expressions, valid at low and high frequencies, are provided for the upstream, downstream and total sound power. A study of the effects of chord length on the total sound power at all reduced frequencies is presented. The isolated airfoil model presented in this paper will subsequently be used as a benchmark to study the effects of cascade in broadband interaction noise of fans.

I. INTRODUCTION

This paper presents the results of a study of the sound power (per unit span) due to an isolated 2D flat plate airfoil in a turbulent stream. The model for sound power presented in this study is to be subsequently compared with the 2D cascade interaction noise model due to Cheong et al. [1], where the unsteady blade loading is computed numerically, in order to study the effects of cascade on interaction broadband noise of fans. The derivation of sound power presented in this report extends the classical results of Amiet [2] to a 2D problem. This problem has been first addressed by Atassi et al. [3], who used numerical schemes to compute the unsteady pressure jump across the flat plate, but further insight into the physics is presented in this paper by using analytical expressions for the unsteady blade loading due to the impingement of a turbulent gust. The characteristics of the incoming turbulence are expressed in terms of the Liepmann turbulent velocity spectrum, for the sake of consistency with the model by Cheong et al. [1]. The airfoil response to the turbulent upwash is expressed in terms of the analytical response functions due to Amiet [4, 5].

Three main results are shown in this paper. First, the "switch" condition introduced by Amiet [2] for the use of either a low frequency or the high frequency flat-plate response function is refined in order to remove possible discontinuities in the noise spectrum, which can occur at low observer angles. Analytical asymptotic expressions, valid at low and high frequency, of the sound power per unit span are then derived. Finally, the effects of the airfoil chord length on the sound power are investigated for the full range of reduced frequency. Three different scaling laws of the sound power with the airfoil chord are identified.

II. POWER SPECTRAL DENSITY OF THE BROADBAND NOISE RADIATED FROM A 2D FLAT PLATE

This section presents an expression for the power spectral density (PSD) of the broadband noise due to the impingement of homogeneous and isotropic turbulence on the leading edge of a 2D flat plate airfoil. This model extends the classical result of Amiet [2] for a 3D airfoil to a 2D airfoil (see Fig. 1). A derivation of the PSD similar to the one of this section, but for a skewed isolated airfoil and where the pressure jump Δp is computed numerically, can be found in Ref. [3].

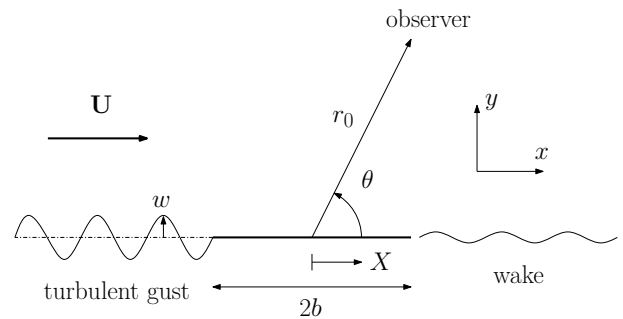


Figure 1: Configuration of the 2D problem of turbulence-flat plate interaction noise.

First, the homogeneous and isotropic turbulent velocity field is assumed to be a "frozen" velocity pattern as it passes the leading edge of the flat plate, and the upwash turbulent velocity can therefore be written as

$$w(X, t) = \frac{1}{2\pi} \int_{-\infty}^{\infty} \mathcal{W}(k_X) e^{-ik_X(X-Ut)} dk_X, \quad (1)$$

where \mathcal{W} is the upwash velocity in the wavenumber domain and is defined in a frame moving with the base flow as

$$\mathcal{W}(k_X) = \int_{-\infty}^{\infty} w(X) e^{ik_X X} dX. \quad (2)$$

For a single harmonic vortical gust, with upwash velocity of the form $w_0 e^{-k_X(X-Ut)}$, the pressure jump is given by

$$\Delta p(X, t) = 2\pi\rho_0 U w_0 g(X, k_X, M) e^{ik_X U t}, \quad (3)$$

where $M = U/c_0$ and $g(X, k_X, M)$ is the non-dimensional transfer function between the turbulent upwash velocity and the pressure jump. In this study, the flat plate response functions g derived by Amiet [4, 5] are used, following the same approach as in Ref. [6], while setting the spanwise wavenumber to zero in order to consider a fully 2D problem. The complete expression of the unsteady pressure jump, in the time domain,

is obtained by combining Eqs. 1 and 3 as

$$\Delta p(X, t) = \rho_0 U \int_{-\infty}^{\infty} \mathcal{W}(k_X) g(X, k_X, M) e^{ik_X U t} dk_X. \quad (4)$$

The unsteady pressure jump in the frequency domain can be deduced from Eq. 4 as

$$\begin{aligned} \Delta \hat{p}(X, \omega) &= \int_{-\infty}^{\infty} \Delta p(X, t) e^{-i\omega t} dt, \\ &= 2\pi \rho_0 \mathcal{W}(K_X) g(X, K_X, M), \end{aligned} \quad (5)$$

where $K_X = \omega/U$. Considering that the surface of the flat plate is rigid, the radiated acoustic pressure due to the unsteady pressure jump Δp is given from Green's theorem by

$$p(x, y, t) = \frac{-1}{2\pi} \int_{-\infty-b}^{\infty} \int_{-\infty}^b \Delta \hat{p}(X, \omega) \frac{\partial G}{\partial y}(x, y, X, \omega) e^{i\omega t} dX d\omega. \quad (6)$$

The 2D Green's function, with effects of mean flow, is given by

$$G(x, y, X, \omega) = \frac{-ie^{ik_0 M(x-X)/\beta^2}}{4\beta} H_0^{(2)}\left(\frac{k_0}{\beta^2} \sqrt{(x-X)^2 + \beta^2 y^2}\right), \quad (7)$$

where $k_0 = \omega/c_0$, $\beta = \sqrt{1-M^2}$ and where $H_0^{(2)}$ is the Hankel function of the second kind and of order 0. The derivative of Eq. 7 with respect to y is given by

$$\begin{aligned} \frac{\partial G}{\partial y}(x, y, X, \omega) &= \frac{iy e^{ik_0 M(x-X)/\beta^2}}{4\beta \sqrt{(x-X)^2 + \beta^2 y^2}} \\ &\times H_1^{(2)}\left(\frac{k_0}{\beta^2} \sqrt{(x-X)^2 + \beta^2 y^2}\right). \end{aligned} \quad (8)$$

Assuming that the observer is in the far-field, the Hankel function $H_1^{(2)}$ and the flow-corrected distance between source and observer $(x-X)^2 + \beta^2 y^2$ can be approximated, respectively, as

$$H_1^{(2)}(\zeta) \approx \sqrt{\frac{2}{\pi\zeta}} e^{-i\zeta + i3\pi/4}, \quad (9)$$

$$(x-X)^2 + \beta^2 y^2 \approx \sigma - \frac{Xx}{\sigma}, \quad (10)$$

where $\sigma = \sqrt{x^2 + \beta^2 y^2}$. Considering that the second term of Eq. 10 can be neglected in amplitude terms, substituting Eqs. 9 and 10 into Eq. 8 leads to the far-field approximation

$$\frac{\partial G}{\partial y}(x, y, X, \omega) = \frac{iy}{4} \sqrt{\frac{2k_0}{\pi\sigma^3}} e^{-i\frac{k_0}{\beta^2}[\sigma - Xx/\sigma - M(x-X)] + i\frac{3\pi}{4}}. \quad (11)$$

The PSD of the acoustic pressure is given by

$$S_{pp}(x, y, \omega) = \int_{-\infty}^{\infty} \langle p^*(x, y, t) p(x, y, t + \tau) \rangle e^{-i\omega\tau} d\tau, \quad (12)$$

where the brackets $\langle \cdot \rangle$ represent the ensemble average. Substi-

tuting Eq. 6 into 12 yields after some algebra

$$\begin{aligned} S_{pp}(x, y, \omega) &= \frac{1}{2\pi} \int_{-\infty}^{\infty} \int_{-b}^b \int_{-\infty}^b S_{QQ}(X_1, X_2, \omega_1, \omega_2) e^{i(\omega_1 - \omega_2)t} \\ &\times \frac{\partial G^*}{\partial y}(x, y, X_1, \omega_1) \frac{\partial G}{\partial y}(x, y, X_2, \omega_2) \delta(\omega - \omega_2) dX_1 dX_2 d\omega_1 d\omega_2. \end{aligned} \quad (13)$$

The cross-spectrum of the unsteady pressure jump S_{QQ} between two points X_1 and X_2 of the plate surface is written as

$$\begin{aligned} S_{QQ}(X_1, X_2, \omega_1, \omega_2) &= \langle \Delta \hat{p}^*(X_1, \omega_1) \Delta \hat{p}(X_2, \omega_2) \rangle \\ &= (2\pi \rho_0)^2 \langle \mathcal{W}^*(K_{X1}) \mathcal{W}(K_{X2}) \rangle \\ &\times g^*(X_1, K_{X1}, M) g(X_2, K_{X2}, M), \end{aligned} \quad (14)$$

where $K_{X1} = \omega_1/U$ and $K_{X2} = \omega_2/U$.

Assuming homogeneous turbulence, setting $X_2 - X_1 = \delta X$ and using the definition of the upwash velocity spectrum yields

$$\begin{aligned} \langle \mathcal{W}^*(K_{X1}) \mathcal{W}(K_{X2}) \rangle &= 2\pi \delta(K_{X1} - K_{X2}) \int_{-\infty}^{\infty} e^{iK_{X2} \delta X} \\ &\times \langle w(X_1) w(X_1 + \delta X) \rangle d\delta X \\ &= 2\pi \delta(K_{X1} - K_{X2}) \Phi_{ww}(K_{X2}), \end{aligned} \quad (15)$$

where Φ_{ww} is the 1D velocity spectrum of the turbulent upwash. The Liepmann 1D turbulent velocity spectrum is used here for consistency with the model of Ref. [1], to which the current model will be compared in subsequent work, and is given by

$$\Phi_{ww}(K_X) = \frac{\overline{u^2} L}{2\pi} \frac{1 + 3K_X^2 L^2}{(1 + K_X^2 L^2)^2}. \quad (16)$$

The final expression for the PSD of the acoustic pressure radiated to the far-field is obtained by substituting Eqs. 11, 14 and 15 into Eq. 13 to give

$$S_{pp}(x, y, \omega) = \frac{\pi \rho_0^2 b^2 y^2 U k_0}{2\sigma^3} \Phi_{ww}(K_X) |\mathcal{L}(x, y, K_X)|^2, \quad (17)$$

where \mathcal{L} is a non-dimensional unsteady loading term defined as

$$\mathcal{L}(x, y, K_X) = \frac{1}{b} \int_{-b}^b g(X, K_X, M) e^{i\frac{k_0}{\beta^2}(M-x/\sigma)X} dX. \quad (18)$$

Since the main interest of this study is sound power, it is convenient to express the location of the far field observer in polar coordinates (r_0, θ) . Equations. 17 and 18 can, therefore, be rewritten as

$$S_{pp}(r_0, \theta, \omega) = \frac{\pi \rho_0^2 b^2 \sin^2 \theta U k_0}{2r_0 A(\theta, M)^3} \Phi_{ww}(K_X) |\mathcal{L}(\theta, K_X)|^2, \quad (19)$$

where the notation $A(\theta, M) = \sqrt{1 - M^2 \sin^2 \theta}$ has been introduced for the sake of brevity, and where

$$\mathcal{L}(\theta, K_X) = \frac{1}{b} \int_{-b}^b g(X, K_X, M) e^{i\frac{k_0}{\beta^2} \left(M - \frac{\cos \theta}{A(\theta, M)}\right) X} dX. \quad (20)$$

Following the approach of Amiet [6], the unsteady loading term \mathcal{L} is defined differently depending on the value of a chord-based acoustic reduced frequency $\mu_a = \frac{\omega b}{c_0 \beta^2} = \frac{K_X M b}{\beta^2}$.

If $\mu_a < \pi/4$, the Sears-like flat-plate response function introduced in ref. [4] is used and Eq. 20 becomes

$$\mathcal{L}_{low}(\theta, K_X) = \frac{1}{\beta} S(\mu_h) e^{i\mu_h f(M)} \left\{ J_0 \left(\mu_a M \frac{\cos\theta}{A(\theta, M)} \right) - iJ_1 \left(\mu_a M \frac{\cos\theta}{A(\theta, M)} \right) \right\}, \quad (21)$$

where J_0 and J_1 are Bessel functions of the first kind, S is the well known Sears function (Ref. [7]), $f(M) = (1 - \beta) \ln M + \beta \ln(1 + \beta) - \ln(2)$, and a chord-based hydrodynamic reduced frequency has been introduced as $\mu_h = \frac{\omega b}{U\beta^2} = \frac{\mu_a}{M}$.

If $\mu_a > \pi/4$, the high frequency response function due to Amiet [5] is used and Eq. 20 becomes

$$\mathcal{L}_{high}(\theta, K_X) = \mathcal{L}_1(\theta, K_X) + \mathcal{L}_2(\theta, K_X), \quad (22)$$

where the functions \mathcal{L}_1 and \mathcal{L}_2 represent the leading edge scattering and the trailing-edge back-scattering of the sound, respectively, and are given by

$$\mathcal{L}_1(\theta, K_X) = \frac{\sqrt{2}}{\pi\beta\sqrt{\mu_h(1+M)}\Theta_1} E^*(2\Theta_1) e^{i\Theta_2}, \quad (23)$$

$$\mathcal{L}_2(\theta, K_X) = \frac{e^{i\Theta_2}}{\pi\Theta_1\beta\sqrt{2\pi\mu_h(1+M)}} \left[i \left(1 - e^{-i2\Theta_2} \right) + (1-i) E^* \left(4\mu_a\beta^2 \right) - \sqrt{\frac{2}{1 + \frac{\cos\theta}{A(\theta, M)}}} E^*(2\Theta_3) \right], \quad (24)$$

where the conjugate of the Fresnel integral $E^*(z)$ is defined as

$$E^*(z) = \frac{1}{\sqrt{2\pi}} \int_0^z \frac{e^{-i\zeta}}{\sqrt{\zeta}} d\zeta, \quad (25)$$

and where the following notations have been introduced for the sake of brevity

$$\Theta_1 = \mu_a \left(1 - \frac{\cos\theta}{A(\theta, M)} \right), \quad (26)$$

$$\Theta_2 = \beta^2 \mu_h + \mu_a \left(M - \frac{\cos\theta}{A(\theta, M)} \right), \quad (27)$$

$$\Theta_3 = \mu_a \left(1 + \frac{\cos\theta}{A(\theta, M)} \right). \quad (28)$$

The validity of Amiet's approach for "switching" between \mathcal{L}_{low} and \mathcal{L}_{high} , depending on the value of μ_a , is discussed in section IV. and refinements of the "switch" condition are introduced.

III. ANALYTICAL FORMULATION FOR SOUND POWER

In practical applications, such as the prediction of fan broadband noise from aircraft engines, it is generally of interest to predict separately the upstream and downstream sound power. In this section, an analytical expression is derived for the total sound power \mathcal{P} , from which the expressions for the upstream and downstream sound power (noted \mathcal{P}^+ and \mathcal{P}^- , respectively) are deduced.

The general definition of the time averaged acoustic intensity vector \mathbf{I} in an isotropic potential flow with uniform velocity is given by (see for instance Morfey [8])

$$\mathbf{I} = \overline{p\mathbf{u}} + \frac{\mathbf{M}}{\rho_0 c_0} \overline{p^2} + \mathbf{M} \overline{p(\mathbf{u} \cdot \mathbf{M})} + \rho_0 c_0 \overline{\mathbf{u}(\mathbf{u} \cdot \mathbf{M})} \quad (29)$$

where $\mathbf{M} = \mathbf{U}/c_0$ is the Mach number vector of the mean flow, p is the acoustic pressure fluctuation, \mathbf{u} is the acoustic velocity fluctuation vector and the upper bar denotes the time average.

The sound intensity I_R in the direction of the observer can be deduced from Eq. 29 as

$$I_R(r_0, \theta, \omega) = \frac{1}{2} \text{Re} \left\{ \hat{p} \hat{u}_R^* + \frac{M \cos\theta}{\rho_0 c_0} |\hat{p}|^2 + M^2 \cos\theta \hat{p} \hat{u}_x^* + M \rho_0 c_0 \hat{u}_R \hat{u}_x^* \right\}, \quad (30)$$

where \hat{u}_R and \hat{u}_x are the frequency domain components of the acoustic velocity fluctuations in the radial and the streamwise directions respectively. The coordinates (r_0, θ, ω) have been omitted in the right hand side for the sake of brevity.

The acoustic velocities \hat{u}_R and \hat{u}_x can be expressed as a function of the far-field pressure spectrum \hat{p} by, first, considering the velocity potential defined as

$$p(r_0, \theta, t) = -\rho_0 \left(\frac{\partial}{\partial t} + U \frac{\partial}{\partial x} \right) \Phi(r_0, \theta, t), \quad (31)$$

which gives in the frequency domain

$$\hat{p}(r_0, \theta, \omega) = -i\rho_0 c_0 \left(k_0 - iM \frac{\partial}{\partial x} \right) \Phi(r_0, \theta, \omega). \quad (32)$$

Equation 32 can be rewritten by use of the chain rule, and after some algebra, as

$$\hat{p}(r_0, \theta, \omega) = -i\rho_0 c_0 k_0 \frac{A(\theta, M) - M \cos\theta}{\beta^2 A(\theta, M)} \Phi(r_0, \theta, \omega). \quad (33)$$

The acoustic velocity fluctuations in the radial and polar directions are expressed from the definition of the velocity potential as

$$\hat{u}_R(r_0, \theta, \omega) = \frac{\partial \Phi(r_0, \theta, \omega)}{\partial r_0}, \quad (34)$$

$$\hat{u}_\theta(r_0, \theta, \omega) = \frac{1}{r_0} \frac{\partial \Phi(r_0, \theta, \omega)}{\partial \theta}. \quad (35)$$

The acoustic velocity fluctuation in the axial directions is derived from the above as

$$\hat{u}_x(r_0, \theta, \omega) = \hat{u}_R(r_0, \theta, \omega) \cos\theta - \hat{u}_\theta(r_0, \theta, \omega) \sin\theta. \quad (36)$$

Substituting equations 34 to 36 into Eq. 33 and considering only the solutions of order $O(1/r_0)$ yields the direct relation between acoustic velocities and pressure

$$\hat{u}_R(r_0, \theta, \omega) = A(\theta, M) \frac{\hat{p}(r_0, \theta, \omega)}{\rho_0 c_0}, \quad (37)$$

$$\hat{u}_x(r_0, \theta, \omega) = \left(A(\theta, M) \cos\theta - M \sin^2\theta \right) \frac{\hat{p}(r_0, \theta, \omega)}{\rho_0 c_0}. \quad (38)$$

The expression of the time averaged sound intensity in the direction of the observer is then obtained by substituting Eq. 37 and Eq. 38 into 30 as

$$I_R(r_0, \theta, \omega) = \frac{|\hat{p}(r_0, \theta, \omega)|^2}{2\rho_0 c_0} F(\theta, M), \quad (39)$$

where the function $F(\theta, M)$ is defined by

$$F(\theta, M) = \frac{\beta^4 A(\theta, M)}{(A(\theta, M) - M \cos\theta)^2}. \quad (40)$$

The above analysis shows that the acoustic intensity towards the observer, with effects of mean flow, can be obtained from the PSD of the acoustic pressure multiplied by a function $F(\theta, M)$,

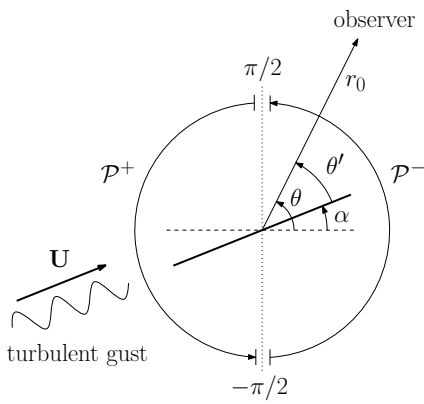


Figure 2: Configuration for upstream and downstream power calculation for a 2D airfoil with stagger angle α .

given by Eq. 40. The total sound power per unit span is then obtained by integrating the expected value of Eq. 39 over a cylinder of unit height, of center $(r_0, \theta) = (0, 0)$, radius r_0 and elemental length $dl = r_0 d\theta$ to give

$$\mathcal{P}(\omega) = \frac{r_0}{2\rho_0 c_0} \int_0^{2\pi} S_{pp}(r_0, \theta, \omega) F(\theta, M) d\theta. \quad (41)$$

Substituting Eq. 19 into 41 finally yields

$$\begin{aligned} \mathcal{P}(\omega) &= \frac{\pi}{4} \beta^4 M k_0 \rho_0 b^2 \Phi_{ww}(K_X) \\ &\times \int_0^{2\pi} \frac{|\mathcal{L}(\theta, K_X)|^2 \sin^2 \theta}{A(\theta, M)^2 (A(\theta, M) - M \cos \theta)^2} d\theta. \end{aligned} \quad (42)$$

It is generally of interest, for ducted turbofan, to predict separately the sound power radiated upstream and downstream of the duct, denoted respectively by \mathcal{P}^+ and \mathcal{P}^- . Equation 42 is therefore extended to allow predictions of \mathcal{P}^\pm , which must be sensitive to variations in stagger angle α . As shown in Fig. 2, the expression for the upstream and downstream power \mathcal{P}^\pm can be deduced from the expression of the total power $\mathcal{P} = \mathcal{P}^+ + \mathcal{P}^-$ by making the change of variables $\theta' = \theta - \alpha$ and integrating between $-\pi/2$ and $\pi/2$. Equation 42 is therefore modified as

$$\begin{aligned} \mathcal{P}^\pm(\omega) &= \frac{\pi}{4} \beta^4 M k_0 \rho_0 b^2 \Phi_{ww}(K_X) \\ &\times \int_{\mp\pi/2}^{\pm\pi/2} \frac{|\mathcal{L}(\theta', K_X)|^2 \sin^2 \theta'}{A(\theta', M)^2 (A(\theta', M) - M \cos \theta')^2} d\theta'. \end{aligned} \quad (43)$$

The total sound power level in dB, as a one-sided function of angular frequency, can therefore be computed as

$$PWL(\omega) = 10 \log_{10} \left(\frac{2\mathcal{P}(\omega) \Delta R}{10^{-12}} \right), \quad (44)$$

where a factor 2 is introduced to take into account the negative frequencies and where ΔR is the airfoil span.

IV. REFINED CONDITION FOR THE "SWITCH" BETWEEN INCOMPRESSIBLE AND COMPRESSIBLE RESPONSE FUNCTIONS

Since there is no analytical flat plate response function g (in Eq. 20) valid at all frequencies, Amiet introduced in Ref. [2] a critical acoustic reduced frequency $\mu_a = \pi/4$ below which

the low frequency incompressible solution (Eq. 21) is used and above which the high frequency compressible solution (Eq. 22) is used. The condition $\mu_a = \pi/4$ physically means that the "switch" between the two solutions occurs when the flow-corrected acoustic wavelength is equal to a quarter of the airfoil chord. This approach is meant to provide a nearly closed analytical solution of the interaction noise problem but is valid only if the functions \mathcal{L}_{low} and \mathcal{L}_{high} are continuous in the neighborhood of $\mu_a = \pi/4$. A check for this continuity is performed in this section and extensions for the condition $\mu_a = \pi/4$ are proposed.

First, the value $\mu_a = \pi/4$ is considered small enough so that the Bessel functions in Eq. 21 can be approximated to unity. Using the approximation $S(\zeta) \approx 1/\sqrt{1+2\pi\zeta}$ (see for instance Ref. [3]), \mathcal{L}_{low} can then be approximated at $\mu_a \approx \pi/4$ as

$$\mathcal{L}_{low}(\theta, K_X) \approx \frac{1}{\beta} \sqrt{\frac{M}{M+2\pi\mu_a}} e^{i\mu_a f(M)/M}. \quad (45)$$

The behaviour of $\mathcal{L}_{high} = \mathcal{L}_1 + \mathcal{L}_2$ at the "switch" condition $\mu_a = \pi/4$ can be investigated by considering the low frequency asymptotic expressions for \mathcal{L}_1 and \mathcal{L}_2 . Using the low argument asymptotic expression of the conjugate Fresnel integral

$$E^*(\zeta) = \sqrt{\frac{2}{\pi}} \sqrt{\zeta} e^{-i\zeta} (1 + \mathcal{O}(\zeta)), \quad (46)$$

the low frequency asymptotic expression for \mathcal{L}_1 and \mathcal{L}_2 are deduced from Eqs. 23 and 24, respectively, as

$$\lim_{\omega \rightarrow 0} \mathcal{L}_1(\theta, K_X) = \sqrt{\frac{M}{1+M}} \sqrt{\frac{8}{\pi^3 \mu_a}} e^{i(\Theta_2 - 2\Theta_1)}, \quad (47)$$

and

$$\begin{aligned} \lim_{\omega \rightarrow 0} \mathcal{L}_2(\theta, K_X) &= \sqrt{\frac{M}{1+M}} \frac{e^{i\Theta_2}}{\mu_a \left(1 - \frac{\cos \theta}{A(\theta, M)}\right)} \\ &\times \left[\frac{i(1 - e^{-i2\Theta_1})}{\sqrt{2\pi^3 \mu_a}} + \frac{2}{\pi^2} (1-i) e^{-i4\mu_a} (\beta^2 e^{iM^2} - 1) \right]. \end{aligned} \quad (48)$$

Note that Eq. 48 presents the factor $1/\left(1 - \frac{\cos \theta}{A(\theta, M)}\right)$ as an amplitude term, whereas no dependency on the observer angle θ is observed in Eqs. 45 and 47. The presence of this factor implies that the low frequency asymptotic expression of the term \mathcal{L}_2 tends to infinity as the observer angle tends to zero. This non-physical behaviour comes from the fact that the decoupling of the leading-edge and the trailing-edge solutions, as $\mathcal{L}_{high} = \mathcal{L}_1 + \mathcal{L}_2$, is not valid at low frequencies. According to Landahl [9] more terms would be needed to capture the complete behaviour of \mathcal{L} at low frequencies, i.e. $\mathcal{L} = \mathcal{L}_1 + \mathcal{L}_2 + \mathcal{L}_3 + \dots$. This becomes an issue because non-physical discontinuities can appear in the noise predictions when the observer angle θ is small and when μ_a approaches $\pi/4$, as shown in Fig. 3 (a).

In order to deal with this issue, a refined condition for the "switch" between the compressible and incompressible solutions is introduced as $\mu_a = \frac{\pi}{4(1 - \cos \theta / A(\theta, M))}$. Using this refined

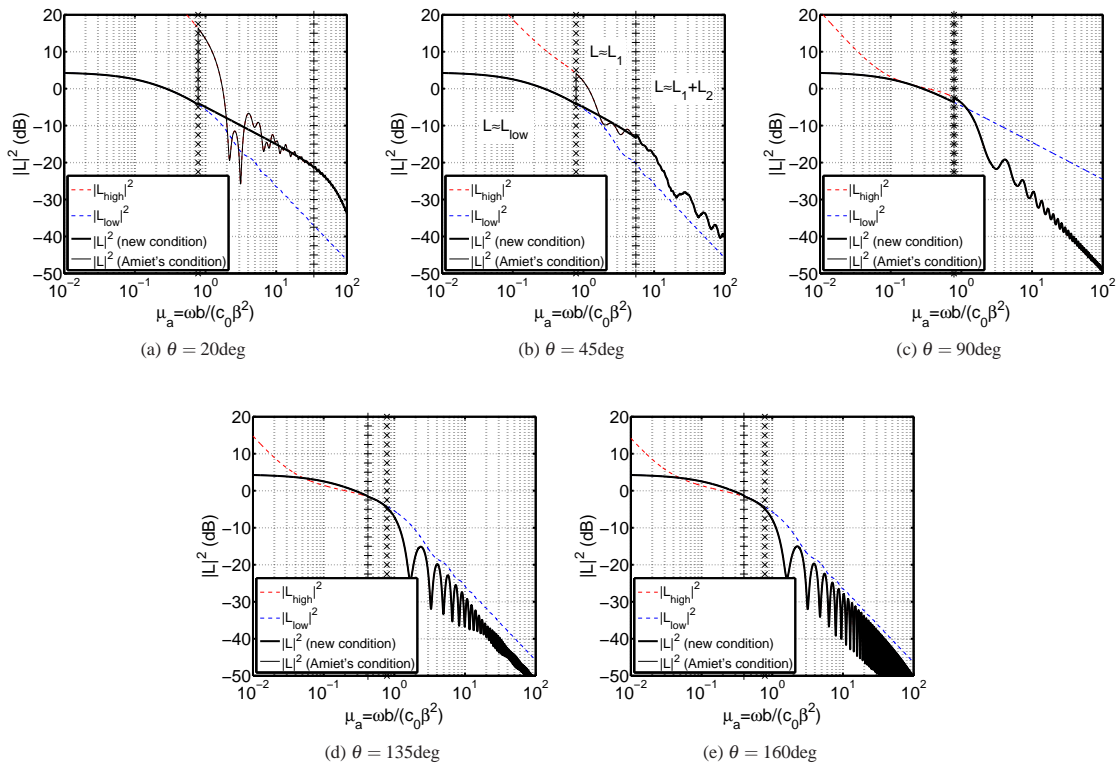


Figure 3: $|\mathcal{L}|^2$ (in dB) as a function of μ_a using Amiet's condition (\times) and the new condition ($+$) for the "switch" between incompressible and compressible response function. $M = 0.8$ and (a) $\theta = 20\text{deg}$, (b) $\theta = 45\text{deg}$, (c) $\theta = 90\text{deg}$, (d) $\theta = 135\text{deg}$ and (e) $\theta = 160\text{deg}$.

condition, the solution for \mathcal{L} is therefore defined as

$$\mathcal{L}_{low} \quad \text{for } \mu_a < \frac{\pi}{4}, \quad (49)$$

$$\mathcal{L}_{high} \approx \mathcal{L}_1 \quad \text{for } \frac{\pi}{4} < \mu_a < \frac{\pi}{4 \left(1 - \frac{\cos\theta}{A(\theta, M)}\right)}, \quad (50)$$

$$\mathcal{L}_{high} \approx \mathcal{L}_1 + \mathcal{L}_2 \quad \text{for } \mu_a > \frac{\pi}{4 \left(1 - \frac{\cos\theta}{A(\theta, M)}\right)}. \quad (51)$$

Figure 3 shows the variation of $|\mathcal{L}|^2$ with μ_a using the new "switch" condition and the "switch" condition used by Amiet [2], for several observer angles, $M = 0.8$ and $b = 0.1$. It appears that the new condition for the "switch" between incompressible and compressible response functions prevents the discontinuities that can otherwise appear in the spectrum of $|\mathcal{L}|^2$ at low θ . The physical reason for this is still under investigation.

V. HIGH AND LOW FREQUENCY ASYMPTOTIC EXPRESSIONS FOR SOUND POWER

V.1. Total sound power

In this section, asymptotic expressions for the total sound power are derived from Eq. 42 in the low and high frequency limit. First, the turbulent velocity spectrum Φ_{ww} , given in Eq. 16, exhibits asymptotic behaviour in the limits of low and high $k_X L$ as

$$\lim_{k_X L \rightarrow 0} \Phi_{ww} = \frac{\overline{u^2} L}{2\pi}, \quad (52)$$

$$\lim_{k_X L \rightarrow \infty} \Phi_{ww} = \frac{\overline{u^2} L}{2\pi} \frac{3}{(k_X L)^2}. \quad (53)$$

Furthermore, from Eqs. 21 to 24, the term $|\mathcal{L}|^2$ exhibits asymptotic behaviour in the limit of low and high acoustic reduced frequency μ_a as

$$\lim_{\mu_a \rightarrow 0} |\mathcal{L}|^2 = \frac{1}{\beta^2} |S(\mu_h)|^2, \quad (54)$$

$$\lim_{\mu_a \rightarrow \infty} |\mathcal{L}|^2 = \frac{1}{\beta^2 \pi^2 \mu_h \mu_a (1+M) \left(1 - \frac{\cos\theta}{A(\theta, M)}\right)}. \quad (55)$$

Note that Eq. 55 is only valid for $\theta \neq 2\pi$. Noting from the definition of the Sears function (Ref. [7]) that $\lim_{\zeta \rightarrow 0} S(\zeta) = 1$ and substituting Eqs. 52 to 55 into 42 yields

$$\lim_{\omega \rightarrow 0} \mathcal{P}(\omega) = \frac{\beta^2}{8} M k_0 \rho_0 b^2 \overline{u^2} L \int_0^{2\pi} d_{low}(\theta, M) d\theta, \quad (56)$$

$$\lim_{\omega \rightarrow \infty} \mathcal{P}(\omega) = \frac{3\beta^6 M \rho_0 \overline{u^2}}{8\pi^2 L K_X^3} \int_0^{2\pi} d_{high}(\theta, M) d\theta, \quad (57)$$

where

$$d_{low}(\theta, M) = \frac{\sin^2\theta}{A^2 (A - M \cos\theta)^2}, \quad (58)$$

$$d_{high}(\theta, M) = \frac{\sin^2\theta}{A^2 (A - M \cos\theta)^2 (1+M) \left(1 - \frac{\cos\theta}{A}\right)}, \quad (59)$$

and where $A(\theta, M)$ has been abbreviated to A , for the sake of brevity.

The functions d_{low} and d_{high} represent the directivity of the acoustic intensity in the direction of the observer in the low and high frequency limit, respectively. Note that the directivity

functions d_{low} and d_{high} tend in the low Mach number limit to

$$\lim_{M \rightarrow 0} d_{low}(\theta, M) = \sin^2 \theta, \quad (60)$$

$$\lim_{M \rightarrow 0} d_{high}(\theta, M) = \sin^2 \frac{\theta}{2}, \quad (61)$$

which is in agreement with the classical result stating that, in the low Mach number limit, interaction noise presents the directivity of a dipole at low frequency and of a cardioid at high frequency (see for instance Ref. [10]). The integrals over d_{low} and d_{high} in Eqs. 56 and 57 can be computed analytically to give

$$\int_0^{2\pi} d_{low}(\theta, M) d\theta = 2\pi \frac{1-\beta}{M^2 \beta^4}, \quad (62)$$

$$\int_0^{2\pi} d_{high}(\theta, M) d\theta = \frac{2\pi}{\beta^6}. \quad (63)$$

The final asymptotic expressions for the total sound power (per unit span) in the low and high frequency limits are therefore obtained by substituting Eqs. 62 and 63 into Eqs. 56 and 57 to give

$$\lim_{\omega \rightarrow 0} \mathcal{P}(\omega) = \rho_0 c_0^2 k_0 b^2 M I_t^2 L \frac{\pi(1-\beta)}{4\beta^2}, \quad (64)$$

$$\lim_{\omega \rightarrow \infty} \mathcal{P}(\omega) = \rho_0 c_0^2 M^3 I_t^2 \frac{3}{4\pi L K_X^3}, \quad (65)$$

where $I_t = \sqrt{u'^2}/U^2$ is the turbulence intensity. Note that, in the low Mach number limit, Eq. 64 is consistent with the low reduced frequency expression of Atassi et al. [3] (Eq. 43), where ρ_0 , b and Φ_{ww} were set to unity. However, unlike the expression of Atassi et al., the low frequency asymptotic expression for sound power given in Eq. 64 is valid at any Mach number and provides an absolute estimation of the sound power, since the low frequency asymptote of the Liepmann velocity spectrum is included.

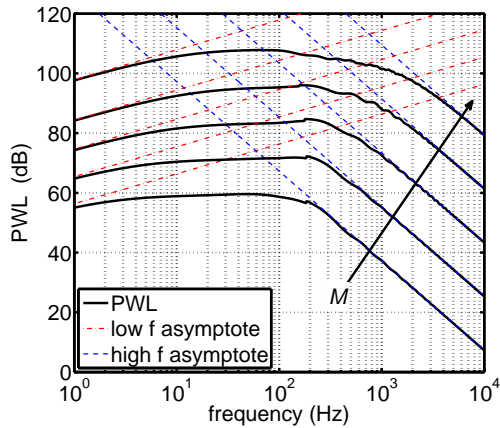


Figure 4: Predicted PWL and low and high frequency asymptotes for $M = 0.05, 0.1, 0.2, 0.4, 0.8$.

Figure 4 presents a comparison, for several values of M , of the general expression for sound power level given in Eq. 42 with the asymptotic expressions given in Eqs. 64 and 65. The input parameters used are the same used in Ref. [2], i.e. an airfoil with a span of $\Delta R = 53.34\text{cm}$ and a half-chord of $b = 22.86\text{cm}$, a turbulent integral lengthscale of $L = 3.175\text{cm}$ and turbulent intensity of $\sqrt{u'^2}/U = 4.4\%$. The air density and speed of sound are set to $\rho_0 = 1.2$ and $c_0 = 340\text{m}\cdot\text{s}^{-1}$. The results shown in

Fig. 4 validate the asymptotic expressions for sound power per unit span derived in this section.

V.2. Upstream and downstream sound power

Similarly to the results shown for the total sound power \mathcal{P} in the previous section, it is possible to derive analytical asymptotic expressions for \mathcal{P}^\pm from Eq. 43 in the limits of low and high frequency. By integrating Eqs. 56 and 57 over θ according to Fig. 2, the low and high frequency asymptotic expressions for the upstream and downstream sound power are given by

$$\lim_{\omega \rightarrow 0} \mathcal{P}^\pm(\omega) = \frac{\beta^2}{8} M k_0 \rho_0 b^2 \overline{u'^2} L \int_{\mp\pi/2}^{\mp\pi/2} d_{low}(\theta', M) d\theta, \quad (66)$$

$$\lim_{\omega \rightarrow \infty} \mathcal{P}^\pm(\omega) = \frac{3\beta^6 M \rho_0 \overline{u'^2}}{8\pi^2 L K_X^3} \int_{\mp\pi/2}^{\mp\pi/2} d_{high}(\theta', M) d\theta. \quad (67)$$

Using the definitions of d_{low} and d_{high} (Eqs. 58 and 59, respectively), analytical solutions for the integrals in Eqs. 66 and 67 can be obtained and substituted in Eqs. 66 and 67 to give the final asymptotic expressions for the upstream and downstream power as

$$\lim_{\omega \rightarrow 0} \mathcal{P}^\pm(\omega) = \rho_0 c_0^2 k_0 b^2 M I_t^2 L \frac{f_{low}^\pm(\alpha, M)}{4\beta^2}, \quad (68)$$

$$\lim_{\omega \rightarrow \infty} \mathcal{P}^\pm(\omega) = \rho_0 c_0^2 M^3 I_t^2 \frac{3f_{high}^\pm(\alpha, M)}{4\pi^2 L K_X^3}, \quad (69)$$

where the non-dimensional functions f_{low}^\pm and f_{high}^\pm are given by

$$f_{low}^\pm(\alpha, M) = \frac{\pi}{2} (1-\beta) \mp \sin^{-1}(M \cos \alpha) \pm M \cos \alpha \sqrt{1 - M^2 \cos^2 \alpha}, \quad (70)$$

$$f_{high}^\pm(\alpha, M) = \pi H(\mp 1) \pm \cos^{-1}(M \cos \alpha) \mp \cos \alpha \sqrt{1 - M^2 \cos^2 \alpha}, \quad (71)$$

and where $H(\mp 1)$ is the Heaviside step function of argument ∓ 1 , which is thus equal to 0 in the upstream case and 1 in the downstream case. As expected, the sum of the downstream and the upstream version of the asymptotic expression for \mathcal{P}^\pm (Eqs. 68 and 69) yields the asymptotic expression for the total sound power \mathcal{P} (Eqs. 64 and 65).

Figure 5 presents a comparison, for $M = 0.2$ and 0.8 and $\alpha = 0^\circ, 30^\circ$ and 60° , of the general expression for sound power level given in Eq. 42 with the asymptotic expressions given in Eqs. 68 and 69. The configuration used is the same as the one presented in section V.1. As expected, the asymptotic expressions for \mathcal{P}^\pm agree well with the predictions made using the exact Eq. 43 in the low and high frequency limits.

The functions f_{low}^\pm and f_{high}^\pm , introduced in Eqs. 70 and 71, represent the effects of stagger angle on \mathcal{P}^\pm . Figure 6 shows the variation of the functions f_{low}^\pm and f_{high}^\pm , normalised by $(f_{low}^+ + f_{low}^-)/2 = \frac{\pi}{2}(1-\beta)$ and $(f_{high}^+ + f_{high}^-)/2 = \frac{\pi}{2}$, with stagger angle α , for different Mach numbers. It appears that the difference between the upstream and downstream expression of f_{low}^\pm and f_{high}^\pm decays with α and is eventually null at $\alpha = 90^\circ$. This is due to the fact that the directivity of the interaction noise is symmetrical with the chord of the flat plate. Note also that, as expected, all the sound power is radiated downstream when $\alpha = 0$ and $M = 1$.

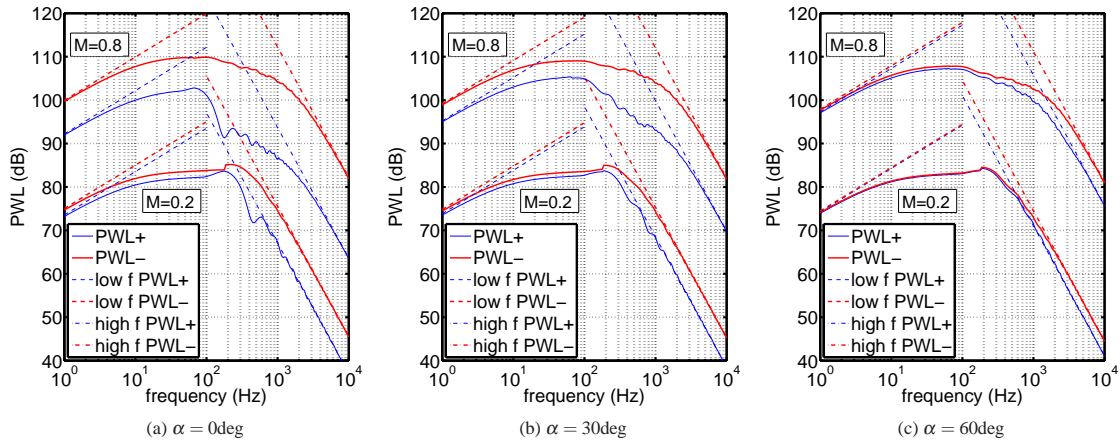


Figure 5: Predicted upstream and downstream PWL and low and high frequency asymptotes for $M = 0.2, 0.8$ and (a) $\alpha = 0^\circ$, (b) $\alpha = 30^\circ$ and (c) $\alpha = 60^\circ$.

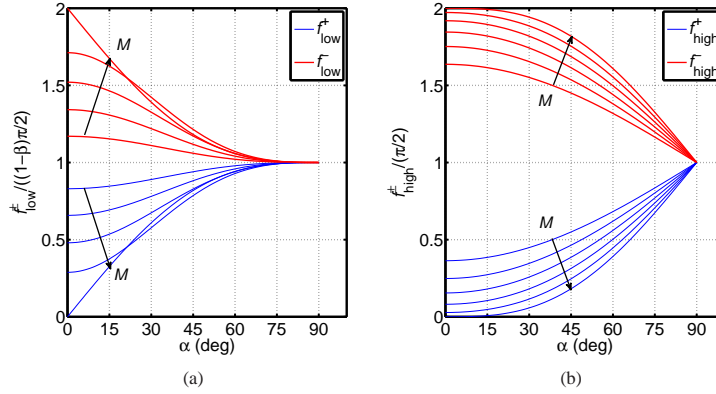


Figure 6: Variation of (a) $f_{low}^{\pm} / (\frac{\pi}{2}(1-\beta))$ and (b) $f_{high}^{\pm} / \frac{\pi}{2}$ with α , for $M = 0, 0.2, 0.4, 0.8, 1$.

VI. EFFECTS OF CHORD LENGTH ON SOUND POWER

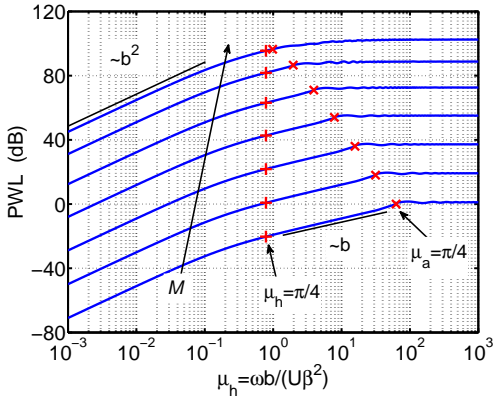


Figure 7: Effect of chord length on PWL for $M = 0.0125, 0.025, 0.05, 0.1, 0.2, 0.4, 0.8$. $\mu_h = \frac{\pi}{4}$ is marked by a + and $\mu_a = \frac{\pi}{4}$ is marked by a \times .

The effects of chord length on sound power level are controlled only by the airfoil response function and vary depending on the value of the acoustic and hydrodynamic reduced frequencies, $\mu_a = \frac{\omega b}{c_0 \beta^2}$ and $\mu_h = \frac{\omega b}{U \beta^2}$. Figure 7 presents the variation

of PWL with μ_h , varying b , keeping ω fixed and for a range of Mach numbers. The same input parameters described in section V.1 are used. The scaling of PWL with the half chord b is different in three distinct ranges of reduced frequency μ_h . The physical meaning of the low, medium and high reduced frequency ranges is described below and represented in Fig. 8.

First, when $(\mu_h, \mu_a) \ll \pi/4$, the wavelength of the vortical gust (i.e. the hydrodynamic wavelength) and the acoustic wavelength are large compared to a quarter of the chord $2b$ of the flat plate. The noise sources on the flat plate surface can, therefore, be considered as compact dipoles which radiate coherently along the chord, hence the b^2 scaling observed in Fig. 7. This behaviour is proved mathematically in section V., where the low frequency asymptotic expressions of sound power (Eq. 64) clearly scales with b^2 .

When $(\mu_h, \mu_a) \gg \pi/4$, the hydrodynamic and the acoustic wavelength are small compared to a quarter of the chord $2b$ of the flat plate. The response of a flat plate of finite chord can, therefore, be approximated by the response of a semi-infinite flat plate ($\mathcal{L} \approx \mathcal{L}_1$). Thus, the effects of finite chord length are negligible in the limit of high hydrodynamic and acoustic reduced frequencies and PWL is independent of b , as observed in Fig. 7. This behaviour is also proved mathematically in section V., where the high frequency asymptotic expressions of sound power (Eq. 65) do not depend on b .

Note that the low and high frequency scalings of the leading

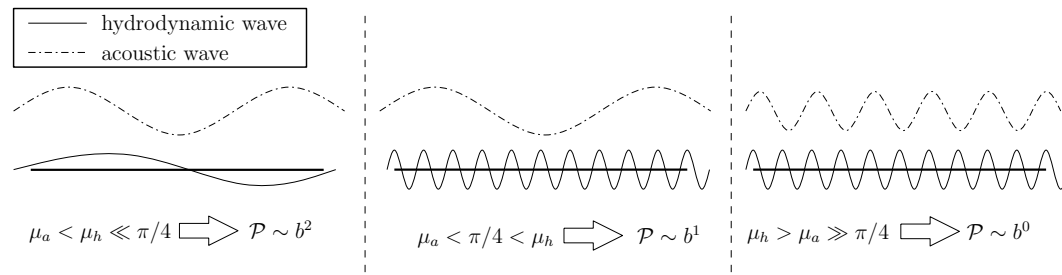


Figure 8: Physical representation of the low, medium and high reduced frequency ranges of the effects of chord length.

edge noise have been first observed by Amiet [11], for the case of turbulence ingestion in a rotor and for the sound pressure level perceived by an observer on the rotor axis. The present results confirm those findings using analytic asymptotic expressions for sound power level.

In the sub-range $\mu_a < \pi/4 < \mu_h$, a different scaling of PWL with b is observed. This sub-range, which becomes significantly large at low flow speeds, represents physically the frequencies where the wavelength of the vortical gust is significantly smaller than the acoustic wavelength. In that region, the hydrodynamic wavelength is smaller than a quarter of the chord ($\mu_h > \pi/4$) whereas the acoustic wavelength is larger than a quarter of the chord ($\mu_a < \pi/4$). This phenomenon, therefore, leads to a scaling of PWL with b only, as shown in Fig. 8. This b -scaling arises from equations 45 and 47, which both show that $|\mathcal{L}|^2 \sim b^{-1}$ in the sub-range $\mu_a < \pi/4 < \mu_h$. To the knowledge of the authors, the existence of a mid-frequency band where the sound power scales with b is presented here for the first time.

VII. CONCLUSION

The contributions of this paper are listed as follows :

- Analytical expressions have been derived for the upstream, downstream and total sound power per unit span due to the interaction of a turbulent flow with the leading edge of a 2D flat plate airfoil.
- Amiet's "switch" condition between the low and high frequency airfoil response functions has been refined in order to remove possible discontinuities in the noise spectrum, which can occur at low observer angles.
- Low and high frequency asymptotic expressions for the upstream, downstream and total sound power per unit span have been obtained, where the integral over the observer angle has been solved analytically.
- The scaling of the sound power with the airfoil chord has been established over the full frequency range. It has been shown that PWL scales differently with the half-blade chord b depending on the value of the hydrodynamic and acoustic reduced frequencies. Three scaling laws have been identified as $\text{PWL} \sim b^2$ at low frequencies, $\text{PWL} \sim b^1$ at mid frequencies and $\text{PWL} \sim b^0$ at high frequencies.

The expressions presented in this report are to be compared with a 2D cascade interaction noise model, where the unsteady loading is computed numerically, in order to study the effects of cascade on the interaction noise of fans.

ACKNOWLEDGEMENTS

The authors would like to thank A. B. Parry from Rolls-Royce plc. for suggesting the study of the continuity between the incompressible and compressible flat plate response functions. The research leading to these results has received funding from Rolls-Royce plc. and the European Community's Seventh Frame-

work Programme FP7/2007-2013 under grant agreement n^o 211861 - validation of Radical Engine Architecture systems (DREAM).

REFERENCES

- [1] C. Cheong, P. Joseph, and S. Lee. High frequency formulation for the acoustic power spectrum due to cascade-turbulence interaction. *The Journal of the Acoustical Society of America*, 119(1):108–122, 2006.
- [2] R. K. Amiet. Acoustic radiation from an airfoil in a turbulent stream. *Journal of Sound and Vibration*, 41(4):407–420, 1975.
- [3] H. M. Atassi, M. Dusey, and C. M. Davis. Acoustic radiation from a thin airfoil in nonuniform subsonic flows, *AIAA Journal*. *AIAA Journal*, 31:12–19, 1993.
- [4] R. K. Amiet. Compressibility effects in unsteady thin-airfoil theory. *AIAA Journal*, 12(2):252 – 255, 1974.
- [5] R. K. Amiet. High frequency thin-airfoil theory for subsonic flow. *AIAA Journal*, 14(8):1076–1082, 1976.
- [6] R. K. Amiet. Noise produced by turbulent flow into rotor: Theory manual for noise calculation. Technical Report 181788, NASA, 1989.
- [7] W. J. Sears. Some aspects of non-stationary airfoil theory and its practical applications. *Journal of Aeronautical Sciences*, 8(3):104–108, 1941.
- [8] C. L. Morfey. Acoustic energy in non-uniform flows. *Journal of Sound and Vibrations*, 14(2):159–170, 1971.
- [9] M.T. Landahl. *Unsteady Transonic Flow*. Pergamon Press, 1961.
- [10] M. S. Howe. *Acoustics of fluid-structure interactions*. Cambridge University Press, 1998.
- [11] R. K. Amiet. Noise due to rotor-turbulence interaction. Technical Report 19780024880, NASA, 1978.